Personalized Gait Phase Estimation for Post-Stroke Individuals via Supervised Domain Adaptation with Limited Gait Data

Sanguk Choi[1] and Kyoungchul Kong[1]

Abstract— **Accurate estimation of gait phase is essential for synchronizing wearable robot control with human movement, thereby enhancing both assistance quality and user safety. While deep learning approaches have demonstrated superior performance in estimating continuous gait phase from multimodal sensor signals, their generalizability to impaired populations remains limited due to inter-subject variability, pathological movement patterns, and compensatory strategies such as hip hiking and circumduction. Furthermore, safety and ethical constraints hinder the collection of extensive data from individuals with stroke, posing challenges for training robust models. To overcome these limitations, we propose a personalized gait phase estimation using supervised domain adaptation (SDA) framework. Our method jointly trains a feature extractor and domain-specific regression heads using labeled data from both healthy individuals (source domain) and stroke survivors (target domain), encouraging feature alignment while preserving task-specific accuracy. Experimental results on a combined dataset, including individuals with chronic hemiplegia, demonstrate that the proposed approach outperforms conventional training and data augmentation baselines, achieving high estimation accuracy even with limited target data. This work contributes to the development of adaptive and data-efficient control strategies for wearable robots targeting individuals with gait impairments.**

I. INTRODUCTION

Accurate prediction of gait phase is a crucial component in the control of wearable robots for gait assistance. Real-time recognition of the wearer's gait phase enables the robot to synchronize its assistance with human movement, thereby enhancing both control performance and locomotion safety. For instance, precise phase detection allows the robot to apply assistive torque during appropriate gait intervals or dynamically adjust impedance parameters to meet varying biomechanical demands. As such, gait phase estimation has become a key research challenge in the development of wearable exoskeletons.

The challenge becomes significantly more pronounced when assisting individuals with gait impairments, such as those affected by stroke, cerebral palsy, or Parkinson's disease. Pathological gait patterns are often characterized by asymmetry, inconsistent cadence, and compensatory strategies such as hip hiking, circumduction, and vaulting. These features make phase transitions ambiguous, thereby complicating phase estimation. Furthermore, gait patterns in post-stroke individuals tend to exhibit substantial inter-subject variability, driven by differences in neuromuscular deficits and compensatory mechanisms.

Traditional gait phase estimation methods often rely on heuristic rules and simple thresholding based on signals from wearable sensors such as inertial measurement units (IMUs) and force-sensitive resistors (FSRs). For example, Ding et al. estimated stride timing by detecting the peak hip flexion event using a thigh-mounted IMU, and measured the stride duration as the interval between successive flexion peaks. Nozaki et al. [1] distinguished the stance and swing phases of hemiplegic gait using foot-mounted IMU data, while Kotiadis et al. [2] employed threshold-based techniques to detect terrain-specific gait patterns. However, such methods are typically constrained to specific walking conditions with near-constant cadence and fail to generalize to overground or variable-speed scenarios.

To overcome these limitations, recent studies have explored deep learning-based methods as powerful alternatives for robust gait phase recognition. Unlike rule-based approaches, deep models such as Convolutional Neural Networks (CNNs), Long Short-Term Memory (LSTM) networks, and Transformers can capture complex temporal dynamics and nonlinear features from sensor data. For instance, Hannink et al. [**?**] achieved accurate gait event detection using a CNN-LSTM model trained on wearable IMU data, whilst Yan et al. [**?**] improved prediction accuracy by integrating EMG and IMU signals within an LSTM-based framework.

However, the performance of such models heavily depends on the size, diversity, and domain alignment of training datasets. Public datasets like HuGaDB, PAMAP2, and the OU-ISIR Gait Database have accelerated the development of models for healthy individuals. Yet, their applicability to impaired populations remains limited. Due to safety concerns such as fall risk and fatigue, data collection from post-stroke individuals is restricted, resulting in small and imbalanced datasets [3]. Moreover, the high heterogeneity in pathological gait further hinders model generalization. Consequently, most studies involving post-stroke individuals have focused on detecting discrete gait events (e.g., heel strike) rather than estimating continuous gait phase [4].

A promising solution to these challenges is transfer learning, which enables a model trained on a source domain (e.g., healthy gait data) to adapt to a target domain (e.g., impaired gait data) with limited labeled samples. Techniques such as fine-tuning [**?**], [**?**] and domain adaptation [**?**], [**?**] have been successfully applied in biomedical signal analysis to reduce inter-subject variability or cross-task gaps. For example,

[1] The authors are with the Department of Mechanical Engineering, Korea Advanced Institute of Science and Technology (KAIST), Daejeon 34141, Republic of Korea sangukchoi@kaist.ac.kr; kckong@kaist.ac.kr

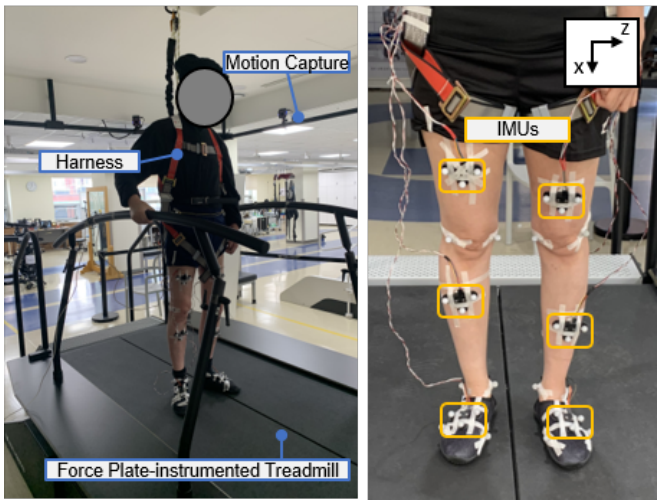

Fig. 1. Experimental setup for collecting post-stroke gait data. (a) Subjects walked on a force plate-instrumented treadmill while wearing a safety harness. (b) The placement of IMUs on the lower limbs and trunk.

Choi et al. [**?**] utilized domain-adversarial neural networks (DANN) for continuous gait phase estimation, but primarily focused on healthy subjects. Despite these advances, few studies have applied domain adaptation specifically for continuous gait phase estimation in post-stroke populations using wearable sensor data.

In this study, we propose a personalized gait phase estimation framework using supervised domain adaptation (SDA) for post-stroke individuals. Unlike previous approaches that rely solely on small target datasets, our method leverages a large dataset of healthy gait (source domain) to learn robust feature representations, which are then adapted to the post-stroke gait (target domain). By minimizing the Maximum Mean Discrepancy (MMD) between the latent features of the two domains, the model aligns the distributions while maintaining regression performance specifically for the target subject.

The primary contribution of this work is the development of a data-efficient deep learning framework tailored to pathological gait analysis. We demonstrate that a model pre-trained on healthy gait data can be effectively adapted to stroke survivors through supervised domain adaptation, achieving high accuracy even with limited patient data. This work provides practical insights into the deployment of deep learning for personalized wearable robot control in rehabilitation.

II. Methods

A. Dataset Construction

To enable accurate gait phase estimation for post-stroke individuals, we constructed a two-domain dataset composed of (1) a publicly available dataset of able-bodied individuals and (2) a post-stroke dataset collected through controlled experiments. The former serves as the source domain, while the latter forms the target domain.

TABLE I

Summary of source and target domain datasets

Property	Source Domain [5]	Target Domain
# of Subjects	22	7
Population	Healthy	Post-stroke
# of Strides per Person	980-1100	40-70

1) Target domain dataset: The target domain dataset was collected from seven individuals with chronic post-stroke hemiparesis (6 males, 1 female; height: 173.3 ± 5.6 cm; body mass: 69.6 ± 11.2 kg). All participants provided written informed consent, and the experimental protocol was approved by the Institutional Review Board (IRB) of the Korea Advanced Institute of Science and Technology (KAIST). Subjects were instructed to walk on a treadmill at three speeds: their self-selected preferred speed, a slower speed (90% of the preferred speed), and a faster speed (110% of the preferred speed). Each subject completed three trials, one per speed condition, with over 50 strides recorded per condition. To ensure safety during treadmill walking, all participants wore a safety harness throughout the experiment as shown in Fig. 1. IMU data were collected from seven anatomical locations—bilateral thigh, shank, foot, and trunk segments—at a sampling frequency of 1000 Hz. The collected IMU signals were then downsampled to 100 Hz to synchronize with the motion capture system and to match the sampling rate of the source domain. The trunk IMU signal was acquired using the onboard sensor integrated into the NI myRIO data acquisition system, while the remaining six locations (bilateral thigh, shank, and foot) used MPU-6050 modules (TDK InvenSense). Additionally, synchronized motion capture and ground reaction force (GRF) data were recorded at 100 Hz.

2) Source domain dataset: The source domain dataset is derived from the publicly available dataset published by Camargo et al. [5], which includes motion capture and wearable sensor data (IMU, EMG, and goniometer) from 22 able-bodied participants. The dataset covers multiple locomotor tasks, including treadmill walking, overground walking, stair ambulation, and ramp traversal under various conditions. For this study, we extracted IMU data from the thigh segment during treadmill walking trials at multiple speeds. This subset was selected to match the sensor configuration and locomotion context used in the target domain, facilitating effective domain adaptation. The sensor data were originally recorded at 200 Hz. To ensure temporal consistency with the target dataset, the source dataset was uniformly downsampled to 100 Hz.

Table I summarizes the physical characteristics of participants in both the source and target domains.

B. Sensor Selection and Data Pre-processing

Post-stroke hemiplegic gait typically presents greater impairments in distal joints compared to proximal ones [6]. To minimize the domain gap between healthy individuals and

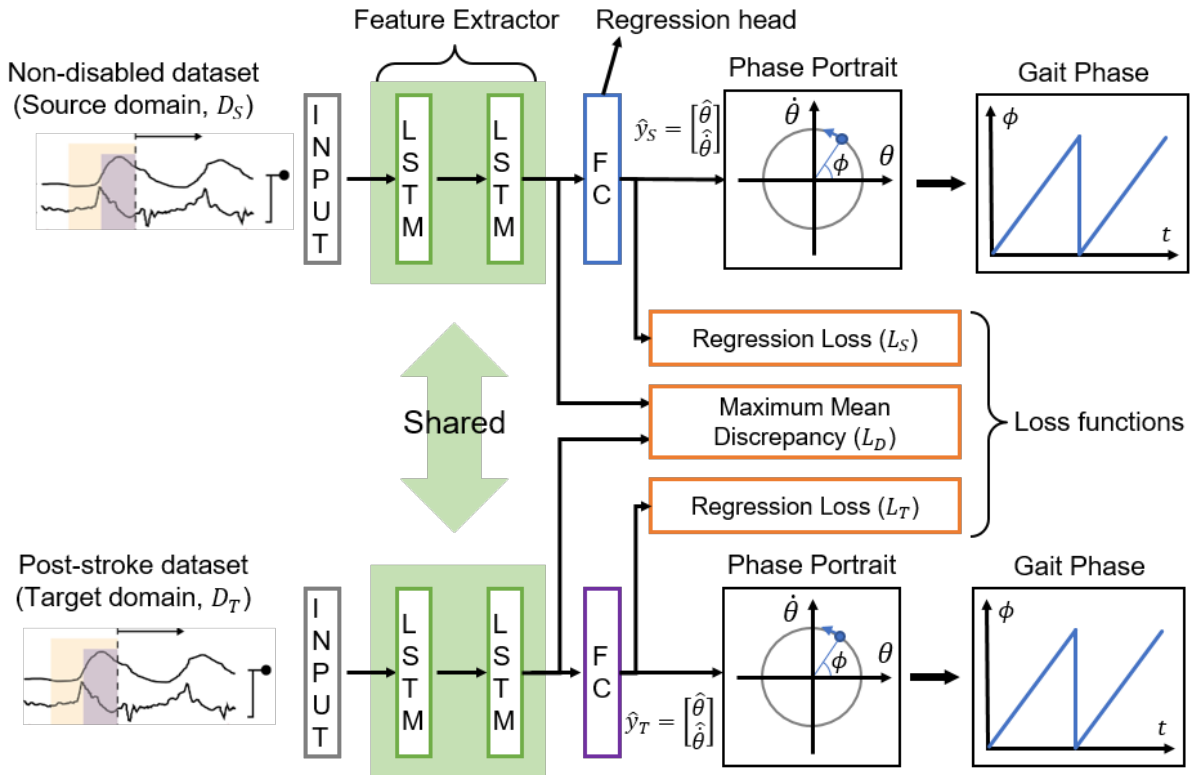

Fig. 2. Proposed framework for gait phase estimation via supervised domain adaptation. A shared LSTM feature extractor learns from both source and target domains, while domain-specific regressors predict continuous gait phase values. MMD loss is used to align the latent feature distributions across domains during training.

post-stroke patients, this study utilizes IMU data acquired from the paretic thigh, a proximal joint.

The input features include raw 3-axis acceleration and angular velocity signals from the thigh-mounted IMU on the paretic side, as well as the estimated thigh angle and angular velocity in the sagittal plane. The angle is estimated using a complementary filtering approach that combines accelerometer- and gyroscope-based estimates. Specifically, the accelerometer-derived angle, $\hat{\theta}_a$, is computed using the arctangent of acceleration components, while the gyroscope-derived angle, $\hat{\theta}_g$, is obtained via numerical integration of angular velocity.

Given that accelerometers are more reliable at low frequencies and gyroscopes at high frequencies, the complementary filter is designed accordingly. The low-pass filter $G(z)$ applied to θ_a is defined as:

$$G(z) = \frac{T_s \omega_c}{1 + T_s \omega_c - z^{-1}}, \tag{1}$$

where T_s denotes the sampling period and ω_c is the cutoff frequency. The corresponding high-pass filter applied to θ_g is given by $\bar{G}(z) = 1 - G(z)$. The final estimate of the thigh angle is computed as:

$$\hat{\theta}(z) = G(z)\theta_a + \bar{G}(z)\theta_g. \tag{2}$$

The cutoff frequency of the complementary filter is set to 1.0 Hz, which was empirically determined to effectively separate the low-frequency drift of the accelerometer from the high-frequency noise of the gyroscope.

The ground truth gait phase was determined using vertical ground reaction force (vGRF) data recorded from each dataset. Heel strike events were identified when the vGRF signal exceeded a threshold of 10% of the subject's body weight, indicating initial foot contact with the ground. Consecutive heel strikes of the same foot defined the boundaries of a gait cycle. Within each cycle, the gait phase ϕ was assigned as a continuous, normalized time variable monotonically increasing from 0 to 1. Specifically, the phase value was defined as $\phi = \frac{t - t_i}{t_{i+1} - t_i}$, where t denotes the current time, and t_i and t_{i+1} represent the timestamps of two successive heel strikes.

A total of eight sensor-derived features are used as inputs to the neural network, structured into a 2-dimensional matrix using a sliding time window. Each input window spans 500 ms (50 samples at 100 Hz sampling rate), capturing temporal dependencies within the gait cycle. Prior to being fed into the network, all input features are standardized to have zero mean and unit variance (Z-score normalization) to ensure stable convergence during training.

C. Gait Phase Estimation Model via Supervised Domain Adaptation

1) Framework Overview: We formulate gait phase estimation as a regression task that maps multivariate time-series sensor input $\mathbf{x} \in \mathbb{R}^{50\times 8}$ to a continuous representation

of gait phase, where the input window length is 50 and the number of features is 8. To handle the discontinuity inherent at the gait cycle boundary, we adopt a phase portrait representation [7]. The gait phase ϕ is converted into angle and angular velocity as expressed as $\theta = cos(2\pi\phi)$ and $\dot{\theta} = sin(2\pi\phi)$, respectively, where $theta \in [0,1)$. Therefore, the output of the gait phase estimation model is derived as

$$y = \begin{bmatrix} \theta \\ \dot{\theta} \end{bmatrix} = \begin{bmatrix} cos(2\pi\phi) \\ sin(2\pi\phi) \end{bmatrix}. \tag{3}$$

The proposed model consists of a shared temporal feature extractor and an independent regression head. The feature extractor comprises multiple stacked Long Short-Term Memory (LSTM) layers, followed by a fully connected layer. The LSTM is a recurrent neural network (RNN)-based architecture in which the estimated variables are retained in the network's internal memory and contribute to the prediction of future time steps. Due to its ability to capture long-term temporal dependencies, the LSTM has demonstrated strong performance in regression tasks involving time-series data [**?**]. Only the final hidden state of the last LSTM layer is used to represent the temporal dynamics, which is then mapped to a 2-dimensional output representing the phase portrait. To prevent overfitting and enhance generalization, we incorporate batch normalization and dropout layers within the network.

To improve generalization across subject groups, we adopt a supervised domain adaptation (SDA) framework. Specifically, datasets from healthy individuals are designated as the source domain $\mathscr{D}_S = (\mathbf{x}_i^S, \mathbf{y}_i^S)_{i=1}^{N_S}$, and datasets from stroke survivors are used as the target domain $\mathscr{D}_T = (\mathbf{x}_j^T, \mathbf{y}_j^T)_{j=1}^{N_T}$, where $N_S \gg N_T$. Unlike traditional two-stage fine-tuning approaches, our framework trains the model jointly on both domains from the start. The feature extractor is shared between domains, allowing the model to learn domain-invariant representations while being supervised by labels from both domains.

Various domain discrepancy measures have been proposed, including Maximum Mean Discrepancy (MMD), Correlation Alignment (CORAL), and adversarial training-based approaches such as Domain-Adversarial Neural Networks (DANN). Among these, MMD is a widely adopted, kernel-based non-parametric measure that quantifies the distance between two probability distributions by comparing the means of their embeddings in a reproducing kernel Hilbert space (RKHS). In this study, we adopt MMD as the domain alignment objective due to its stability, simplicity, and effectiveness in scenarios with limited target domain data. Unlike adversarial approaches that require careful tuning of competing losses or CORAL that aligns only second-order statistics, MMD enables explicit minimization of distributional gaps in a theoretically grounded manner. Furthermore, it does not require domain labels and can be seamlessly integrated into the end-to-end training of deep networks, making it well-suited for our supervised domain adaptation setting with small, labeled target datasets.

TABLE II
GRID SEARCH RANGES AND OPTIMIZED VALUES FOR KEY HYPERPARAMETERS

Hyperparameter	**Search Range**	**Optimized Value**
Hidden units (1st/2nd layer)	{64, 128, 256} (Base)	128, 64
Dropout rate	{0.2, 0.3}	0.3
Batch size	{64, 128, 256}	64
Fully connected layer size	{32, 64, 128}	128
Learning rate	{1e-03, 1e-04}	1e-04
Loss weight λ_S (src MSE)	0.3	0.3
Loss weight λ_T (tgt MSE)	1.0	1.0
Loss weight λ_D (MMD)	{0.5, 1.0, 1.5, 2.0}	0.5

2) Loss Functions: The overall training objective integrates two types of losses: regression loss for supervised learning and a domain alignment loss to minimize feature distribution discrepancy between domains. The total loss is defined as:

$$\mathscr{L}_{\text{total}} = \lambda_S \cdot \mathscr{L}_S + \lambda_T \cdot \mathscr{L}_T + \lambda_D \cdot \mathscr{L}_D, \tag{4}$$

where λ_S, λ_T, and λ_D are weighting coefficients for the source regression loss, target regression loss, and domain alignment loss (MMD), respectively.

The regression losses are computed using the Mean Squared Error (MSE) between predicted and ground-truth phase portraits:

$$\mathscr{L}_S = \frac{1}{N_S} \sum_{i=1}^{N_S} \left\| \hat{\mathbf{y}}_i^S - \mathbf{y}_i^S \right\|_2^2, \tag{5}$$

$$\mathscr{L}_T = \frac{1}{N_T} \sum_{i=1}^{N_T} \left\| \hat{\mathbf{y}}_i^T - \mathbf{y}_i^T \right\|_2^2 \tag{6}$$

where N_S and N_T denote the number of training samples in the source and target domains, respectively; $\hat{\mathbf{y}}_i^S$ and $\hat{\mathbf{y}}_i^T$ are the model predictions for the i-th sample in the source and target domains; $\mathbf{y}_i^S$ and $\mathbf{y}_i^T$ are the corresponding ground-truth phase portrait vectors.

To align the feature distributions, the MMD loss is applied to the output of the shared feature extractor—specifically, the LSTM-encoded representations—prior to the regression heads. Let $\mathbf{h}_i^S$ and $\mathbf{h}_j^T$ denote the extracted feature representations from the source and target domains, respectively. The empirical MMD loss is defined as:

$$\mathscr{L}_D = \left\| \frac{1}{N_S} \sum_{i=1}^{N_S} \phi(\mathbf{h}_i^S) - \frac{1}{N_T} \sum_{j=1}^{N_T} \phi(\mathbf{h}_j^T) \right\|_{\mathscr{H}}^2, \tag{7}$$

where $\phi(\cdot)$ is the feature mapping implicitly defined by a Gaussian kernel:

$$k(\mathbf{h}_i, \mathbf{h}_j) = \exp\left(-\frac{|\mathbf{h}_i - \mathbf{h}_j|^2}{2\sigma^2} \right). \tag{8}$$

3) Hyperparameter Tuning: The hyperparameters of the gait phase estimation model were selected through a grid search procedure using the source domain training data and a held-out validation set. The batch size was searched over {64, 128, 256}, and a size of 64 yielded the best validation

performance. The number of hidden units in the first LSTM layer was selected from {64, 128, 256}, with the second layer set to half the size of the first; the configuration of 128 and 64 units was found to be optimal. A dropout rate of 0.3 was selected from the range {0.2, 0.3} to prevent overfitting. The fully connected layer size was chosen as 128 from the candidates {32, 64, 128}.

All LSTM layers employed the *tanh* activation function. The Adam optimizer was used, with the learning rate selected from {1e-03, 1e-04}. A learning rate of 1×10^{-4} was used. For the supervised domain adaptation setting, the loss weighting coefficients were determined via grid search. The MMD loss weight λ_D was selected from {0.5, 1.0, 1.5, 2.0}, with 0.5 yielding the best balance. The regression loss weights were fixed at $\lambda_S = 0.3$ and $\lambda_T = 1.0$ based on preliminary experiments. The training process was conducted for up to 100 epochs, with early stopping applied if the validation loss did not improve for 5 consecutive epochs. The final hyperparameter configuration is summarized in Table II.

D. Baseline Methods

To demonstrate the effectiveness of the proposed gait phase estimation model, we compare its performance against the following baseline methods.

1) Source Only (SO): The **SO** method simulates a model trained exclusively on the source dataset, which contains gait data from non-disabled individuals. This setting reflects a zero-shot inference scenario where no post-stroke data is used for training.

2) Target Only (TO): The **TO** method represents conventional supervised learning using only the target dataset collected from post-stroke individuals. Although it ensures full label supervision in the target domain, the limited amount of target data poses challenges for model generalization.

3) Fine-tuning (FT): The **FT** method fine-tunes a model pre-trained on the source domain using target domain data. The encoder parameters are frozen to preserve generalized feature representations, while only the decoder is updated to adapt to the specific target subject.

III. Results

A. Loss Dynamics During Training

To better understand the training behavior of the proposed supervised domain adaptation framework, we visualized the evolution of each loss component over 100 training epochs, as shown in Fig. 3.

The *Source Regression Loss* and *Target Regression Loss* gradually decrease as the network learns to fit phase labels from both domains. In the early epochs, the source loss exhibits a more rapid decline due to the abundance of labeled source data, while the target loss reduces more slowly, reflecting the limited target data size. The *MMD Loss*, which aligns the latent feature distributions of source and target domains, also shows a steady decrease throughout training. This indicates successful minimization of domain shift in the shared feature space. The *Total Loss*, plotted as a dashed line, aggregates all components and exhibits a smooth

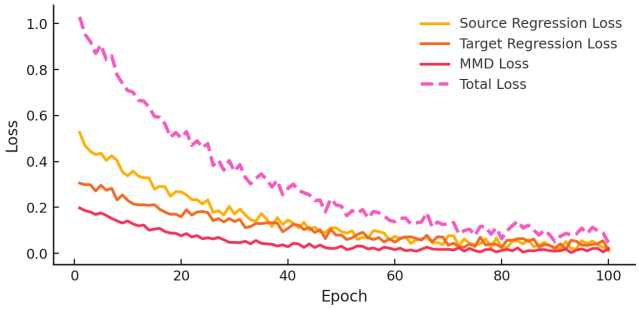

Fig. 3. Training loss components over epochs. Source and target regression losses decrease steadily, while MMD loss ensures domain alignment. Total loss (dashed) is the weighted sum of all components.

downward trend, confirming the stable convergence of the multi-objective training process. These dynamics validate the effectiveness of the proposed loss formulation in balancing regression performance and domain adaptation.

B. Domain Alignment by Supervised Domain Adaptation

To qualitatively evaluate the efficacy of the proposed domain adaptation framework, we visualized the distribution of latent features extracted by the LSTM encoder using t-SNE. Fig. 3 illustrates the feature embedding spaces for six representative post-stroke subjects before and after applying SDA. In the 'Before SDA' case (top row), where the model is trained solely on source data (Source Only), a distinct separation between the source (healthy, blue) and target (stroke, red) domains is observed across all subjects. This clear segregation confirms the existence of a significant domain shift caused by pathological gait patterns, such as asymmetry and compensatory movements, which fundamentally hinders the generalization of a model trained exclusively on healthy data to post-stroke populations.

In contrast, the 'After SDA' case (bottom row) demonstrates a remarkably different landscape. By jointly training with the MMD-based domain alignment loss, the latent feature distributions of the source and target domains become well-aligned and indistinguishably overlapping. This indicates that the shared feature extractor has successfully learned domain-invariant representations that are robust to the kinematic discrepancies between healthy and impaired gait. The successful alignment of these manifolds suggests that the model effectively leverages the rich information from the source domain to compensate for the scarcity of target labels, thereby proving the mechanism behind the performance improvement in gait phase estimation.

C. Gait Phase Estimation Performance

The performance of the proposed supervised domain adaptation method was evaluated against the baseline methods described in the previous section: Source Only (SO), Target Only (TO), and Target with Augmentation (TA). All models were tested on the target domain (i.e., post-stroke individuals) using the same input modality and network architecture to ensure fair comparison.

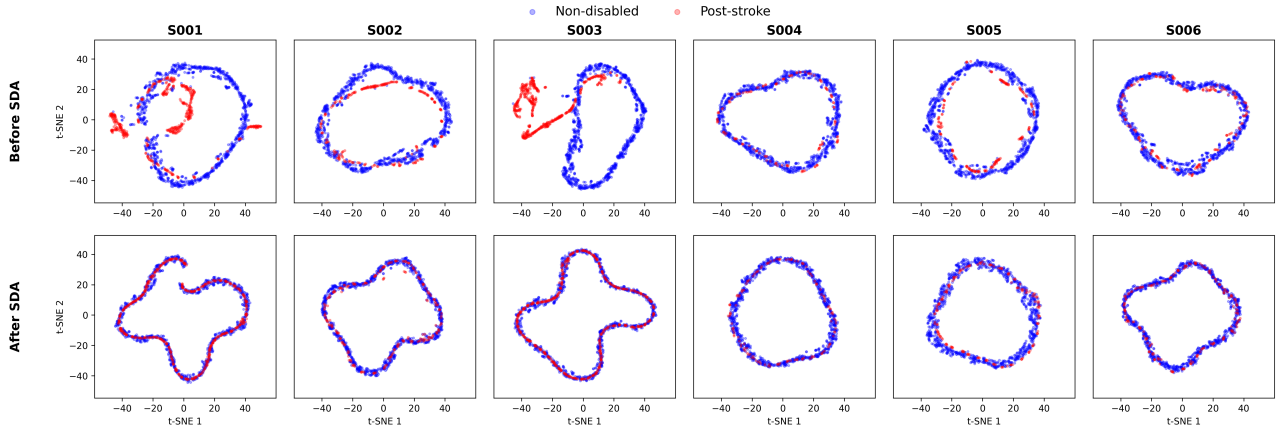

Fig. 4. t-SNE visualization of latent features before and after domain adaptation.

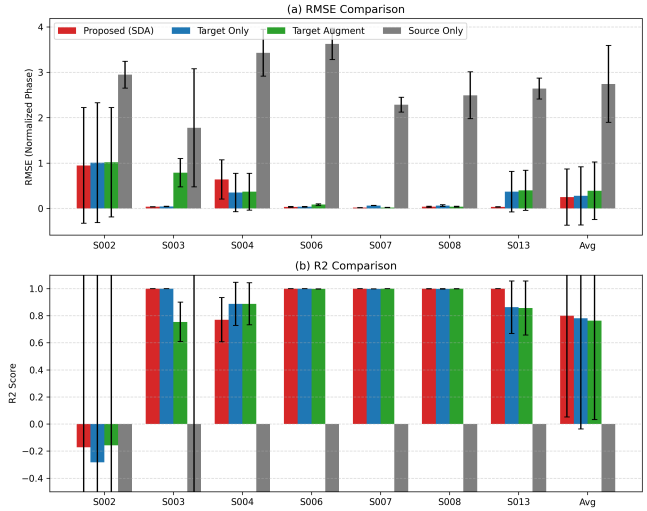

Fig. 5. Gait phase estimation performance evaluated on post-stroke subjects. (a) Root Mean Squared Error (RMSE) in predicted phase. (b) Coefficient of determination (R^2) for regression accuracy.

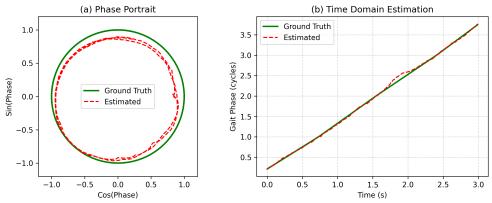

Fig. 6. Gait phase estimation performance evaluated on post-stroke subjects in (a) phase space and (b) time domain.

Fig. 5 illustrates the quantitative results of gait phase prediction for each subject as well as the overall average. In subfigure (a), the Root Mean Squared Error (RMSE) indicates the magnitude of prediction errors, while subfigure (b) presents the R^2 score, which measures how well the predicted phase fits the ground truth.

The proposed method achieved the best performance in both metrics across all subjects. On average, the SDA model achieved an RMSE of 0.039 and an R^2 score of greater than 0.99 for most subjects (S002, S003, S006, S007, S008, S013), significantly outperforming the Source Only (SO) baseline which yielded negative R^2 scores, and improving upon the Target Only (TO) method. While the TA model showed improvements over TO by introducing variability through synthetic augmentation, it still underperformed compared to the proposed SDA method in terms of robustness across different test folds.

These results highlight the benefit of using domain adaptation over naive transfer or data augmentation. Specifically, the proposed framework leverages rich source-domain knowledge while maintaining adaptability to the target domain, enabling more robust and accurate gait phase estimation in individuals with post-stroke gait impairments.

In Fig. 6(a), the phase portrait depicts the relationship between the estimated gait phase $\hat{\phi}$ and its temporal derivative $\dot{\hat{\phi}}$, compared against the ground truth. The ground truth trajectory forms a unit circle centered at the origin, representing an idealized continuous cyclic gait phase. The estimated trajectory closely matches the reference circle, indicating the model's ability to preserve cyclic consistency and temporal smoothness. In Fig. 6(b), the estimated gait phase over time is plotted alongside the ground truth. Both traces exhibit a linear increase from 0 to 1 within each gait cycle, repeating periodically. The close alignment of the two signals demonstrates high accuracy in continuous gait phase prediction.

D. Real-time Inference Evaluation on Edge Device

The estimated gait phase must be applicable to the real-time control of a wearable robot. To evaluate the real-time applicability of the proposed model, we deployed the trained gait phase model on the NVIDIA Jetson Xavier, a high-performance edge device suitable for onboard inference in wearable robotics. The experiment was conducted using the TensorFlow Lite runtime environment in Python. The average inference time for a single sequence was measured as 4.4 ± 1.7 ms, which is sufficiently fast for real-time operation within a 100Hz control loop. Additionally, the peak memory

usage during inference reached 38.6%, indicating that the model can run reliably even within the resource-constrained environment of the Jetson Xavier.

IV. Discussion

(Comparison to SOTA)

V. Conclusion

This study presents a supervised domain adaptation framework for continuous gait phase estimation in individuals with post-stroke hemiplegia. By leveraging labeled datasets from both healthy individuals and stroke survivors, our approach aligns feature representations across domains while maintaining regression performance for each population. Unlike conventional deep learning methods, the proposed SDA method enables more stable and accurate prediction under limited target data conditions, addressing the domain gap induced by pathological gait characteristics. Experimental results confirm that our method significantly improves estimation accuracy over baseline models, particularly in stroke participants with diverse compensatory patterns. These findings demonstrate the potential of SDA-based models to enable personalized, real-time gait phase estimation and lay the groundwork for adaptive control strategies in wearable robotics.

As future work, we plan to (1) integrate the proposed gait phase estimation model into the real-time control loop of a gait assistive exoskeleton to enable phase-synchronized assistance, and (2) extend the framework to other types of pathological gait beyond stroke, such as those caused by cerebral palsy or Parkinson's disease, to evaluate its generalizability and clinical applicability.

References

[1] Y. Nozaki and T. Watanabe, "A basic study on detection of movement state in stride by artificial neural network for estimating stride length of hemiplegic gait using imu," in *2019 41st Annual International Conference of the IEEE Engineering in Medicine and Biology Society (EMBC)*. IEEE, 2019, pp. 3151–3154.

[2] D. Kotiadis, H. J. Hermens, and P. H. Veltink, "Inertial gait phase detection for control of a drop foot stimulator: Inertial sensing for gait phase detection," *Medical engineering & physics*, vol. 32, no. 4, pp. 287–297, 2010.

[3] G. Chen *et al.*, "Gait deviations in patients with stroke: a clustering analysis," *Clinical Rehabilitation*, 2013.

[4] Y. Qian, Y. Wang, H. Geng, H. Du, J. Xiong, Y. Leng, and C. Fu, "Adaptive oscillator-based gait feature extraction method of hip exoskeleton for stroke patients," *IEEE Transactions on Medical Robotics and Bionics*, vol. 6, no. 1, pp. 235–244, 2023.

[5] J. Camargo, A. Ramanathan, W. Flanagan, and A. Young, "A comprehensive, open-source dataset of lower limb biomechanics in multiple conditions of stairs, ramps, and level-ground ambulation and transitions," *Journal of Biomechanics*, vol. 119, p. 110320, 2021.

[6] J. Perry and J. M. Burnfield, *Gait analysis: normal and pathological function*. Slack Incorporated, 2010.

[7] I. Kang, P. Kunapuli, and A. J. Young, "Real-time neural network-based gait phase estimation using a robotic hip exoskeleton," *IEEE Transactions on Medical Robotics and Bionics*, vol. 2, no. 1, pp. 28–37, 2019.